



University  
of Glasgow

Dale, C.W. et al. (2009) *Osmium isotopes in Baffin Island and West Greenland picrites: implications for the  $^{187}\text{Os}/^{188}\text{Os}$  composition of the convecting mantle and the nature of high  $^3\text{He}/^4\text{He}$  mantle*. *Earth and Planetary Science Letters*, 278 (3-4). pp. 267-277. ISSN 0012-821X

<http://eprints.gla.ac.uk/4964/>

Deposited on: 24 February 2009

1 **Osmium isotopes in North Atlantic picrites with extreme  $^3\text{He}/^4\text{He}$  ratios:**  
2 **implications for the nature of high  $^3\text{He}/^4\text{He}$  mantle and the Os isotope**  
3 **composition of the convecting mantle**

4  
5 C.W. Dale<sup>a\*</sup>, D.G. Pearson<sup>a</sup>, N.A. Starkey<sup>b,c</sup>, F.M. Stuart<sup>b</sup>, R.M. Ellam<sup>b</sup>,  
6 L.M. Larsen<sup>d</sup>, J.G. Fitton<sup>c</sup>, C.G. Macpherson<sup>a</sup>

7  
8 <sup>a</sup>*Department of Earth Sciences, Durham University, Science Laboratories, Durham, DH1 3LE, UK*

9 <sup>b</sup>*Isotope Geosciences Unit, SUERC, East Kilbride, G75 0QF, UK*

10 <sup>c</sup>*School of GeoSciences, University of Edinburgh, Edinburgh, EH9 3JW, UK*

11 <sup>d</sup>*Geological Survey of Denmark & Greenland, Ostervoldgade 10 DK, 1350 Copenhagen, Denmark*

12 \*corresponding author. email: [christopher.dale@durham.ac.uk](mailto:christopher.dale@durham.ac.uk). Tel: +44 0191 3342338,

13 Fax: +44 0191 3342301

14 **Abstract**

15 Identifying the Os isotope composition of the prevalent peridotitic convecting mantle places  
16 important constraints on the Earth's accretion, differentiation and evolution. Furthermore, the  
17 accurate interpretation of Re-depletion ages in mantle peridotites is dependent on this composition.  
18 Small degree mantle melts preferentially sample components with the lowest melting temperatures  
19 and so are poorly suited to identifying the Os isotope composition of peridotite components. In  
20 contrast, Os isotope studies of large degree melts such as picrites are much more likely to reflect the  
21 peridotitic components within the source. Thirty proto-Iceland plume picrites from Baffin Island  
22 and West Greenland, produced by large degree mantle melting, have been analysed for Re-Os  
23 isotopes in order to provide an estimate for the bulk  $^{187}\text{Os}/^{188}\text{Os}$  composition of convecting mantle  
24 and to investigate the nature of high  $^3\text{He}/^4\text{He}$  mantle. Ingrowth-corrected  $^{187}\text{Os}/^{188}\text{Os}$  of the picrites  
25 ranges from 0.1267 to 0.1322. The higher  $^{187}\text{Os}/^{188}\text{Os}$  samples have correspondingly lower  
26  $^{143}\text{Nd}/^{144}\text{Nd}$  which may reflect a contribution (~5-10%) from old recycled crust including sediment.  
27 However, samples from Baffin Island and the earliest West Greenland members are remarkably  
28 uniform in composition with  $^{187}\text{Os}/^{188}\text{Os}$  between 0.1267 and 0.1280, and a mode of 0.1272. These  
29 Os isotope compositions are less radiogenic than estimates of PUM but are similar to the least  
30 radiogenic mid-ocean ridge basalts (MORB) and the most common composition of ophiolite-  
31 derived platinum-group alloys and chromites. These compositions appear to represent a source that  
32 contains no significant enriched component such as pyroxenite/eclogite.

33 The picrites studied record the highest known  $^3\text{He}/^4\text{He}$  in the silicate Earth (up to 50  $R_a$ ). For this  
34 signature to reflect isolated domains of ancient melt depletion would require significantly less  
35 radiogenic Os isotope compositions than observed, if mantle Os and He remain coupled.  
36 Conversely, an outer core contribution would impart a supra-chondritic  $^{187}\text{Os}/^{188}\text{Os}$  signature to the  
37 picrites, thus the near-chondritic Os isotope compositions also preclude the core as a source of high

38  $^3\text{He}/^4\text{He}$ , unless the mechanism for transfer of He into the plume is decoupled from that of Os.  
39 However, as the high  $^3\text{He}/^4\text{He}$  signature is found in samples with variable Os and Nd isotope  
40 compositions, it is likely that He is decoupled from other isotopic tracers and is dominated by minor  
41 addition of a He-rich component with high  $^3\text{He}/^4\text{He}$ , probably of primordial nature, although the  
42 ultimate source is unclear. Alternatively, a high  $^3\text{He}/^4\text{He}$  mantle reservoir with  $^{187}\text{Os}/^{188}\text{Os}$  of  
43  $\sim 0.1275$  cannot be ruled out, but the absence of any elevated  $^3\text{He}/^4\text{He}$  in MORB, which has a  
44 similar Os isotope composition, suggests that such a component could only be sampled during  
45 episodes of high degree melting of hot mantle.

46

47 Keywords: osmium isotopes, helium isotopes, Baffin, convecting mantle, depleted mantle.

48

## 49 **1. Introduction**

50 Mantle rocks and mantle-derived melts display a broad range of Os isotope compositions, both  
51 depleted and enriched with respect to bulk Earth and primitive upper mantle (PUM) estimates.

52 Osmium is a compatible element during mantle melting while Re, which is the parent to  $^{187}\text{Os}$   
53 through beta decay of  $^{187}\text{Re}$ , is moderately incompatible. Thus, crustal rocks typically have very  
54 high Re/Os ratios and, over time, evolve to radiogenic  $^{187}\text{Os}/^{188}\text{Os}$  compared to the mantle.

55 Depleted mantle, which has preferentially lost Re over Os, evolves complementary unradiogenic  
56  $^{187}\text{Os}/^{188}\text{Os}$  ratios, with the timing of Re depletion indicated by the extent to which  $^{187}\text{Os}/^{188}\text{Os}$   
57 deviates from a chondritic evolution curve. Therefore, the Re-Os system is a potentially powerful  
58 tool with which to assess the contributions from depleted mantle and enriched recycled materials to  
59 the source of mantle-derived melts.

60 Significant Os isotope heterogeneity exists in the mantle at a variety of length-scales from mineral  
61 to vein to slab scale due to the recycling of enriched crustal materials and depletion of peridotite,  
62 and the highly siderophile nature of both Re and Os. Different degrees of melting of such a  
63 heterogeneous mantle will lead to melts that vary in isotopic composition, with the most radiogenic  
64 melts typically derived from the smallest degrees of melting, and large-degree melts giving the best  
65 estimate of the  $^{187}\text{Os}/^{188}\text{Os}$  composition of the *bulk* mantle source. This study of picrites from  
66 Baffin Island (BI) and West Greenland (WG) should therefore provide a good estimate for the  
67 average Os isotope composition of the source and, given the similarity to depleted MORB mantle in  
68 terms of lithophile isotopes (e.g. Ellam and Stuart, 2004), provide an estimate for the  $^{187}\text{Os}/^{188}\text{Os}$  of  
69 convecting mantle free from enriched components. Such an estimate is a valuable parameter for  
70 constraining the Os isotope evolution of the Earth and peridotite melting ages (e.g. Meisel et al.,  
71 1996; Meisel et al., 2001; Walker et al., 2002b).

72 Mantle  $^3\text{He}/^4\text{He}$  ranges from  $\sim 5$  to  $50 R_a$  (where  $R_a = ^3\text{He}/^4\text{He}_{\text{atmosphere}} = 1.39 \times 10^{-6}$ ) and includes  
73 the canonical mid-ocean ridge basalt (MORB) range of  $8 \pm 1 R_a$  (Graham, 2003). The high  $^3\text{He}/^4\text{He}$   
74 end-member is defined by picrites from Baffin Island (BI) ( $\sim 50 R_a$ , Stuart et al., 2003) and West  
75 Greenland (Graham et al., 1998; Starkey et al., 2007, Starkey et al. in review) which erupted at  
76 about 61 Ma as a result of elevated mantle temperatures and regional rifting due to the arrival of the  
77 Iceland plume (Saunders et al., 1997). Due to the incompatibility of He, conventional wisdom  
78 posits that high  $^3\text{He}/^4\text{He}$  mantle reservoirs are less degassed than the convecting upper mantle, and  
79 retain a component of the Earth's primordial volatile inventory (e.g. Kurz et al., 1982; Moreira et  
80 al., 2001; Porcelli et al., 2002). However, the observation that U and Th may be less compatible  
81 than He in an olivine-rich mantle assemblage has led to the suggestion that high  $^3\text{He}/^4\text{He}$  may result  
82 from the greater loss of U and Th than He during ancient melt depletion (Graham et al., 1990; Class  
83 and Goldstein, 2005; Parman et al., 2005; Parman, 2007). The Re-Os isotope system has the ability  
84 to retain information about mantle melting events, even in the convecting mantle (e.g. Brandon et

85 al., 2000; Meibom et al., 2002; Harvey et al., 2006; Pearson et al., 2007), and thus is the most  
86 suitable tracer to test whether high  $^3\text{He}/^4\text{He}$  signatures can be directly linked to ancient depletion  
87 events.

88 The North Atlantic picrites (NAP) from Baffin Island and West Greenland represent some of the  
89 earliest known volcanic rocks of the proto-Iceland plume, which continues to produce mantle melts  
90 with high  $^3\text{He}/^4\text{He}$  in the Iceland region today (e.g. Macpherson et al., 2005). In this study, Os  
91 isotope data have been (i) combined with existing He and Nd isotope data to re-assess the nature of  
92 the highest known  $^3\text{He}/^4\text{He}$  mantle component, and (ii) used to gain an estimate of the average Os  
93 isotope composition of convecting mantle. The high MgO content of the samples (>15 wt. %) and  
94 correspondingly high Os concentrations mean that they are less susceptible to interactions with  
95 crust and lithospheric mantle – critical when looking at samples which have been erupted through  
96 ancient continental crust and lithosphere.

97

## 98 **2. Samples: setting and chemistry**

99 The high-Mg basalts and picrites in this study were collected from the eastern margin of Baffin  
100 Island (BI) at Cape Searle, Padloping Island and Durban Island and from Disko Island  
101 (Qeqertarsuaq) and the Nuussuaq peninsula in West Greenland (WG). The WG picrites belong to  
102 the Vaigat formation which is divided into three members, from oldest to youngest, the Anaanaa,  
103 Naujánguit and Ordlingassoq Members. The Baffin picrites are undifferentiated stratigraphically  
104 but can be grouped chemically into the enriched (E-type) lavas (DUR-8, DI-23 and PAD-6) and  
105 normal (N-type) lavas (all others) first identified by Francis (1985). Sample CS-7 is from a cross-  
106 cutting dyke, rather than the picrite succession. Volcanism was largely contemporaneous on Baffin  
107 Island and in WG and commenced ~61 Ma (Storey et al., 1998). Both the WG Anaanaa Member

108 and the BI picrites possess normal magnetisation whereas the subsequent WG melts are reversely  
109 magnetised (Pedersen et al., 2002). The whole sequence, and ~80% of the total Paleocene volcanic  
110 rocks, were erupted within 1 million years (Storey et al., 1998). Petrography, major and trace  
111 element chemistry and Sr, Nd and Pb isotopes are described in more detail in previous studies (e.g.  
112 Francis, 1985; Robillard et al., 1992; Holm et al., 1993; Lightfoot et al., 1997; Graham et al., 1998;  
113 Larsen and Pedersen, 2000; Stuart et al., 2003; Kent et al., 2004).

114 MgO contents of the NAP are very high (up to 27 wt. % in this study) which, although in part a  
115 result of olivine accumulation, reflects the Mg-rich nature of parental melts. Estimates for the  
116 parental melts of WG picrites, based on Fo-rich olivine phenocrysts, vary between 15 and 21 wt. %  
117 MgO (Pedersen, 1985; Lightfoot et al., 1997; Graham et al., 1998; Larsen and Pedersen, 2000).  
118 Such high MgO contents in an intra-continental plate setting indicate generation by a high degree of  
119 melting (10-11% depleted mantle, ~20-28% fertile mantle) of anomalously hot mantle (1540-  
120 1600°C) at moderate depths (60-90 km) (Pedersen, 1985; Gill et al., 1992; Herzberg and O'Hara,  
121 2002).

122 The three West Greenland picrite members are largely similar in terms of major elements.  
123 However, for a given MgO content, there is an increase in TiO<sub>2</sub> with time, with the older WG  
124 picrites most closely resembling the Baffin picrites (Holm et al., 1993). Chondrite-normalised REE  
125 patterns are flattest in the Anaanaa and Naujánguit Members (not shown), while the Ordlingassoq  
126 samples have higher LREE and incompatible element concentrations (Holm et al., 1993; Lightfoot  
127 et al., 1997). Neodymium and Sr isotope compositions of the Ordlingassoq picrites appear to  
128 resemble the least depleted Icelandic picrites (Holm et al., 1993).

### 129 3. Analytical techniques and samples

130 Whole rock powders (~1g) were digested and equilibrated with a mixed  $^{190}\text{Os}$ - $^{185}\text{Re}$ -enriched spike,  
131 using inverse aqua regia (2.5 ml 12 mol l<sup>-1</sup> HCl and 5 ml 16 mol l<sup>-1</sup> HNO<sub>3</sub>) in quartz high-pressure  
132 asher (HPA) vessels or borosilicate carius tubes. The HPA vessels were placed in the Durham  
133 University Anton-Paar HPA at 300°C and >110 bars for at least 12 hours, and the Carius tubes were  
134 placed in an oven at 240°C for at least 36 hours. Osmium was extracted using CCl<sub>4</sub>, followed by  
135 back-extraction using HBr, and then microdistilled (Cohen and Waters, 1996). The aqua regia was  
136 dried and prepared for purification of Re using AG1X-8 (100-200#) anion-exchange resin (Pearson  
137 and Woodland, 2000).

138 Osmium was loaded onto Pt filaments, ionised as  $\text{OsO}_3^-$  and analysed by negative-thermal  
139 ionisation mass spectrometry (N-TIMS) using the ThermoFinnigan Triton at Durham University.  
140 All Os isotope beams and mass 233, corresponding to  $^{185}\text{ReO}_3^-$ , were measured sequentially using  
141 an axial secondary electron multiplier. All Os isotope raw data were corrected offline for O isotope  
142 interference, mass fractionation (using a  $^{192}\text{Os}/^{188}\text{Os}$  ratio of 3.08271) and spike unmixing.  
143 Subtraction of a possible  $^{187}\text{ReO}_3^-$  interference was not necessary due to insignificant counts on  
144 mass 233 (<2 cps). Repeated analyses of 170 pg aliquots of the University of Maryland Os  
145 standard solution (UMd, also referred to as UMCP) at Durham University gave  $^{187}\text{Os}/^{188}\text{Os}$  mean  
146 values of  $0.11384 \pm 16$  ( $2\sigma$ , n=19) and  $0.11379 \pm 14$  ( $2\sigma$ , n=39) for the two time periods of analysis,  
147 April 2000 - November 2000 and April 2006 - May 2008, respectively. This is in good agreement  
148 with a value of  $0.113787 \pm 7$  for much larger aliquots (10-100 ng/g) measured on the same mass  
149 spectrometer in Faraday cup mode (Luguet et al., 2008). Rhenium was analysed by inductively-  
150 coupled plasma mass spectrometry (ICP-MS) on a ThermoFinnigan<sup>®</sup> Element 2. Solutions were  
151 introduced using a MicroMist micro-concentric nebuliser and ESI stable sample introduction  
152 system (dual-cyclonic quartz spray chamber). Standard solutions (1 ng/g Re) were analysed at the  
153 start, middle and end of each session to determine mass fractionation.

154 The Carius tube digestions (April 2000 – May 2006) and HPA digestions (November 2007 – May  
155 2008) gave, respectively, mean total procedural blanks of 0.43 and 0.32 pg for Os, 2.5 and 1.9 pg  
156 for Re and  $^{187}\text{Os}/^{188}\text{Os}$  ratios of 0.143 and 0.192. The blank corrections relate to the appropriate  
157 reagent batch rather than a long-term mean, but were always less than 0.1% for concentration and  
158 isotope composition.

159 *Reproducibility of samples.* Duplicate digestions of the same sample powder (n=3) indicate that  
160 reproducibility of  $^{187}\text{Os}/^{188}\text{Os}$  is 0.15% and 0.7% (2 RSD) for an Os-rich (PI-26, ~2 ng/g Os) and  
161 Os-poorer sample (CS-7, 0.46 ng/g), respectively. Os concentrations are reproducible to ~5% (2  
162 RSD) and 11% for PI-26 and CS7, respectively, and Re concentrations (n=2) vary by less than 1%  
163 (2 RSD) for both samples (Re: 0.25 and 0.50 ng/g, respectively). The accuracy of measurements is  
164 more difficult to evaluate, but reproducibility using two different digestion techniques for these  
165 samples and for reference materials (Dale et al., 2008) suggests that incomplete digestion and/or  
166 sample-spike equilibration is unlikely to be a significant consideration.

## 167 **4. Results**

### 168 **4.1 Re and Os elemental data**

169 Osmium concentrations range from 1.50 to 4.02 ng/g in the West Greenland picrites and from 0.435  
170 to 3.45 ng/g in the Baffin Island picrites (Table 1). The median of 2.49 ng/g for the WG suite is  
171 higher than for the Baffin suite (1.66 ng/g). All samples have much greater Os concentrations than  
172 MORB, which have a range of <0.001 to 0.25 ng/g (Roy-Barman and Allegre, 1994; Gannoun et  
173 al., 2007), and the highest Os concentrations are greater than approximate averages for primitive or  
174 depleted mantle (~3.1-3.7 ng/g, Morgan et al., 2001; Becker et al., 2006; Harvey et al., 2006).

175 Rhenium concentrations range from 0.113 to 0.506 ng/g in the BI picrites, with a median of 0.32  
176 ng/g, while the WG samples have a larger range (0.063 to 1.14 ng/g, including two samples with

177 anomalously high Re concentrations from the Anaanaa Member) but a similar median of 0.29 ng/g.  
178 Such Re abundances are lower than MORB (0.34 – 2.28 ng/g, median ~1 ng/g, Schiano et al., 1997;  
179 Sun et al., 2003; Gannoun et al., 2007). There is little overall covariation of Os and Re in the  
180 picrites (not shown), although certain sub-sets, such as samples from Padloping Island, tend to have  
181 increasing Re concentrations with decreasing Os and this is broadly true of the BI picrites as a  
182 whole.

183 Figure 1 here.

184 Osmium concentrations decrease with decreasing MgO (Figure 1) and Ni (not shown). For a given  
185 MgO content, picrites from WG have higher Os abundances than those from Baffin Island, while  
186 Icelandic picrites are lower in Os than all the early plume North Atlantic picrites (NAP) (Brandon et  
187 al., 2007). Rhenium concentrations vary less systematically with MgO content, although a weak  
188 negative co-variation can be seen, particularly in the Baffin samples. With the exception of sample  
189 CS-7, and two Anaanaa (WG) samples with anomalously high Re content, Re/Os ratios tend to  
190 increase with decreasing MgO content in all of the suites (not shown). Re concentrations of  
191 Icelandic picrites are broadly comparable to the NAP, but the lower Os concentrations result in  
192 higher Re/Os ratios in the Iceland suite (Brandon et al., 2007).

193 Table 1 here.

#### 194 **4.2 Os isotope data**

195 Baffin Island picrites have a range of  $^{187}\text{Os}/^{188}\text{Os}$  from 0.1269 to 0.1344, which, when corrected for  
196 ingrowth of  $^{187}\text{Os}$  since the time of emplacement (61 Ma), gives a narrow range of initial  
197  $^{187}\text{Os}/^{188}\text{Os}$  ratios from 0.1267 to 0.1287. The most radiogenic value corresponds to the picrite with  
198 the lowest Os concentration (~0.45 ng/g, Figure 3) and therefore crustal contamination is a likely  
199 mechanism for increasing  $^{187}\text{Os}/^{188}\text{Os}$ . If this value is omitted the range of  $^{187}\text{Os}/^{188}\text{Os}$  is

200 considerably more limited (0.1267 to 0.1278). The WG picrites have a larger range of  $^{187}\text{Os}/^{188}\text{Os}$   
201 and  $^{187}\text{Os}/^{188}\text{Os}_{\text{initial}}$  of 0.1271 – 0.1332 and 0.1267 - 0.1322, respectively. However, the least  
202 radiogenic WG samples form a peak on an initial  $^{187}\text{Os}/^{188}\text{Os}$  probability density plot at 0.12725  
203 (Figure 2), which is indistinguishable from the BI peak (0.12717). The sub-chondritic to supra-  
204 chondritic range of Os isotope values observed in a different suite of BI picrites (Kent et al., 2004)  
205 was not found in this study. Source variability or interaction with lithospheric mantle are both  
206 possible origins for the difference between the BI suites, although Kent et al. (2004) concluded that  
207 the latter was not consistent with other isotope data.

208 The WG picrites analysed here, and by Schaefer et al. (2000), extend to more radiogenic Os isotope  
209 compositions than the BI picrites.  $^{187}\text{Os}/^{188}\text{Os}$  varies with stratigraphy in the Vaigat formation. The  
210 picrites from the Anaanaa and Naujánguit Members possess only the least radiogenic signature  
211 (Figure 3). In contrast,  $^{187}\text{Os}/^{188}\text{Os}$  ratios matching this signature were not found in the slightly  
212 younger Ordlingassoq Member, which instead have initial  $^{187}\text{Os}/^{188}\text{Os}$  of 0.1294 or greater. Such  
213  $^{187}\text{Os}/^{188}\text{Os}$  ratios are more radiogenic than estimates of putative present-day primitive mantle  
214 (0.1296, Meisel et al., 2001) but do not extend as high as WG picrite data from the literature (up to  
215 0.1371, Schaefer et al., 2000). The much younger picrites from Iceland are characterised by more  
216 radiogenic  $^{187}\text{Os}/^{188}\text{Os}$  (up to 0.1378, Brandon et al., 2007) which, in part, may correlate with their  
217 generally lower MgO contents. The main NAP  $^{187}\text{Os}/^{188}\text{Os}$  peak (Figure 2 and Figure 5) is also  
218 significantly less radiogenic than almost all OIB (Figure 5).

219 Figure 2 here.

220 With the possible exception of the sample with the lowest Os concentration, there is no covariation  
221 of  $^{187}\text{Os}/^{188}\text{Os}$  with Os concentration in either Baffin or West Greenland picrites (Figure 3).  
222 Significant assimilation of crust or sub-continental lithospheric mantle (SCLM) would likely result  
223 in samples falling on mixing lines towards either an Os-poor, ancient, extremely radiogenic crustal

224 component or an Os-rich,  $^{187}\text{Os}$ -depleted SCLM; such trends are not observed. Equally, if Os-poor  
225 samples are derived from parental melts with lower Os content, then these melts would be more  
226 susceptible to crustal contamination, and thus are more likely to be radiogenic, and this is not  
227 observed. Previous WG data appear to display increased  $^{187}\text{Os}/^{188}\text{Os}$  with decreasing Os  
228 concentrations (Schaefer et al., 2000). This may indicate crustal assimilation, or possibly  
229 preferential sampling of Os-poorer radiogenic material during mantle melting, for the least Os-rich  
230 samples. However, this is only true for samples with  $<0.5$  ng/g Os; such samples have been omitted  
231 from subsequent figures.

232 Figure 3 here.

## 233 **5. Discussion**

### 234 **5.1 Re-Os elemental behaviour**

235 Olivine accumulation in all the NAP studied is indicated by sample MgO contents of up to 27.0 wt.  
236 %, compared to an estimated parental magma of 18.5-21 wt. % MgO (e.g. Pedersen, 1985; Graham  
237 et al., 1998; Larsen and Pedersen, 2000). Osmium concentrations decrease with decreasing MgO  
238 (Figure 1) and with Ni (not shown), reflecting the compatibility of Os within the olivine- and  
239 sulphide-rich crystallising assemblage, which has previously been recognised in global MORB and  
240 OIB (e.g. Burton et al., 2002). Therefore, Os concentrations are likely controlled by olivine  
241 fractionation and/or accumulation. Rhenium concentrations in the picrites are lower than MORB  
242 which is consistent with the moderate incompatibility of Re during mantle melting and the higher  
243 melt fraction of picritic melts. Re/Yb ratios are comparable to MORB ( $\sim 0.00025$ ). The relative  
244 incompatibility of Re in olivine and associated crystallising phases (e.g. sulphide +/- spinel),  
245 compared to Os, is also illustrated by increasing Re/Os ratios with decreasing MgO content in  
246 almost all the picrite units.

247 As osmium has a very high sulphide-silicate melt partition coefficient (e.g. ~10,000, Crocket et al.,  
248 1997), the estimated Os concentrations for the parental melts of NAP (1-2 ng/g) suggest complete  
249 consumption of sulphides in at least part of the melting column. The consumption of sulphide in a  
250 fertile upper mantle source is thought to occur at melt fractions of >20-25%, based on the sulphide  
251 content of the mantle and sulphur solubility in mafic melts (e.g. Mavrogenes and O'Neill, 1999;  
252 Lorand et al., 2003), or may occur at lower melt fractions given a previously depleted mantle  
253 source. These melt fractions are consistent with estimates based on MgO content: ~20-28% for a  
254 fertile source or 10-11% for a depleted source (Herzberg and O'Hara, 2002). In addition to  
255 sulphide-silicate partitioning, physical entrainment of liquid sulphide within a high-degree silicate  
256 melt (Ballhaus et al., 2006) may, at least in part, account for the very high Os concentration of the  
257 NAP parental melts.

258 West Greenland picrites have higher Os for a given MgO content compared to BI picrites, which  
259 could reflect a greater degree of melting. This has been suggested independently on the basis of  
260 lower MgO content in the Baffin picrites parental melt (Francis, 1985, based on interpretation of  
261 Fo-rich olivines as xenocrysts), although other studies have not concurred with this interpretation  
262 (e.g. Kent et al., 2004). Alternatively, assuming the same degree of melting, a sulphide-poorer  
263 source may result in complete sulphide consumption in a greater proportion of the melting region  
264 and therefore lead to higher Os abundances in melts with similar MgO.

## 265 **5.2 Osmium-neodymium isotope systematics**

266 The majority of NAP analysed here have Nd isotope compositions similar to Icelandic lavas and  
267 consistent with a source dominated by a depleted mantle component ( $^{143}\text{Nd}/^{144}\text{Nd} \sim 0.51307$ ), as  
268 previously noted by Holm et al. (1993). However, none of the picrites are as depleted as estimates  
269 of DMM (Salters and Stracke, 2004; Workman and Hart, 2005), or the depleted end-member of the  
270 Iceland array (e.g. Taylor et al., 1997; Thirlwall et al., 2004). There is considerable  $^{143}\text{Nd}/^{144}\text{Nd}$

271 variation in BI and Anaanaa (WG) picrites, ranging from 0.51273 to 0.51305 (Figure 4; Graham et  
272 al., 1998; Starkey et al., 2007), while  $^{187}\text{Os}/^{188}\text{Os}$  is largely constant at around 0.127. The lower Nd  
273 isotope limit is defined by sample CS7 which appears, on the basis of Os isotopes and a previous  
274 study (Stuart et al., 2003), to contain a crustal component, but even when omitting this sample there  
275 is significant  $^{143}\text{Nd}/^{144}\text{Nd}$  variation. In contrast, the younger Ordlingassoq Member of the WG suite  
276 displays a negative co-variation of Os and Nd isotopes with  $^{143}\text{Nd}/^{144}\text{Nd}$  decreasing from 0.51308 to  
277 0.51291 as  $^{187}\text{Os}/^{188}\text{Os}$  increases from 0.1267 to 0.1322 (Figure 4). The data of Schaefer et al.  
278 (2000), derived from the Naujánguit and Ordlingassoq Members, possess similar systematics to the  
279 Ordlingassoq samples in this study (but not the Naujánguit Member), although the data are more  
280 scattered.

### 281 **5.2.1 Assessing the effects of post-melting crustal or lithospheric interaction**

282 The NAP were erupted through old continental crust, therefore it is important to assess the potential  
283 effects of assimilation of such material. The difficulty in assessing the isotopic effects of such  
284 contamination is that continental crust is markedly heterogeneous in terms of Os (e.g. Peucker-  
285 Ehrenbrink and Jahn, 2001). The Os isotope composition of local crust has not been measured, and  
286 measurements, even if numerous, are unlikely to provide a sufficiently well-constrained average  
287 due to the varied basement geology. Baffin Island basement rocks display a considerable range of  
288  $^{143}\text{Nd}/^{144}\text{Nd}$  and Nd concentrations (Theriault et al., 2001), as do local West Greenland sediments,  
289 which are the most likely contaminants (Larsen, unpubl.). Using assumed Re and Os  
290 concentrations (e.g. Esser and Turekian, 1993; Peucker-Ehrenbrink and Jahn, 2001) and knowledge  
291 of Re-Os behaviour, the Os isotope composition of a possible contaminant has been estimated for  
292 2.5 Ga continental crust, and assimilation of this material has been modelled. Osmium and Re  
293 concentrations of 5, 10, 30 pg/g and 500, 300, 200 pg/g (high Re/Os, best-estimate and low Re/Os,  
294 respectively) have been combined with average Nd concentrations and  $^{143}\text{Nd}/^{144}\text{Nd}$  of 24  $\mu\text{g/g}$  and  
295 0.5109, and 39 and 0.5111 for BI basement and WG metasediments, respectively (Theriault et al.,

296 2001, Larsen, unpubl.). The area defined by possible mixing lines for the entire range of Nd and Os  
297 concentrations and varying Sm/Nd and Re/Os ratios is shown by the grey field in Figure 4.

298 Mixing of parental picritic melt with average/best estimate metasedimentary basement does not  
299 produce either of the data arrays observed (Figure 4). Assimilation cannot produce the observed  
300 variation in  $^{143}\text{Nd}/^{144}\text{Nd}$  without a noticeable change in  $^{187}\text{Os}/^{188}\text{Os}$ . However, mixing of relatively  
301 high Sm/Nd crust could produce the array with Os and Nd isotope co-variation. Mixing curves in  
302 Os-Sr isotope space are also consistent with this conclusion (not shown).

303 On a qualitative level, the observation that Anaanaa and Ordlingassoq samples display different Nd-  
304 Os isotope trends, despite being emplaced in the same region, makes crustal contamination an  
305 unlikely possibility for both trends. However, such a difference could result from changes in  
306 magma plumbing and such stratigraphically variable contamination has been recorded in other  
307 flood-basalt suites (e.g. Thompson et al., 2001). The similarity of major element ( $\text{TiO}_2$ ) and Os-Nd  
308 isotope compositions of Baffin Island and Anaanaa picrites also cannot easily be accounted for by  
309 assimilation. Crust-melt mixing may also result in co-variation of  $^{187}\text{Os}/^{188}\text{Os}$  with Os  
310 concentration (depending on concentrations of contaminant and melt), and this is not observed  
311 (Figure 3).

312 A further and more conclusive line of evidence to suggest that crustal assimilation is not a  
313 significant factor in controlling the isotope compositions of the NAP is presented by Starkey et al.  
314 (2007) and Starkey et al. (in review). The overall trend of increasing Nb/Sm with decreasing  
315  $^{143}\text{Nd}/^{144}\text{Nd}$  in their dataset cannot be accounted for by assimilation of any low-Sm/Nd crustal  
316 material. Very small amounts of crustal contamination can explain the spread in  $^{143}\text{Nd}/^{144}\text{Nd}$ , but  
317 cannot also account for the relative enrichment in incompatible elements. Therefore, Nd isotope  
318 variations (and by inference Os isotopes) appear to be controlled by source heterogeneity of the  
319 mantle.

320 Figure 4 here.

321

### 322 **5.2.2 Generation of the osmium and neodymium isotope variations in the mantle source**

323 The upper part of the Vaigat formation (WG) records increasing  $^{187}\text{Os}/^{188}\text{Os}$  combined with  
324 decreasing  $^{143}\text{Nd}/^{144}\text{Nd}$ . If this cannot be adequately explained by melt-crust interaction, such a  
325 shift to slightly more enriched Os and Nd isotope compositions may reflect an increased input from  
326 an enriched component. For instance, modelled mixing of depleted MORB mantle (DMM) with 2  
327 Ga recycled oceanic crust and associated sediment can produce the negative array in Os-Nd isotope  
328 space (Figure 4, e.g. 5-10% recycled component containing 5-10% sediment). While this model  
329 indicates that recycled oceanic crust and sediments are a plausible contributor, such material is not  
330 necessarily required and it is possible that other enriched material, such as metasomatised oceanic  
331 lithosphere (e.g. Niu and O'Hara, 2003) could produce the negative array.

332 The variation of  $^{143}\text{Nd}/^{144}\text{Nd}$  with no complementary variation of  $^{187}\text{Os}/^{188}\text{Os}$  is more difficult to  
333 explain because old recycled oceanic crust (plus sediment), and old continental crust, both possess  
334 complementary high  $^{187}\text{Os}/^{188}\text{Os}$  and low  $^{143}\text{Nd}/^{144}\text{Nd}$ . However, we suggest that the mantle source  
335 of the Baffin and Anaanaa picrites contained Nd isotope heterogeneity as a result of a minor  
336 (sulphide-poor?) pyroxenite component that, due to its high Nd content and low Os content,  
337 significantly affected the Nd isotope composition of the melt without noticeably affecting Os.

338

### 339 **5.3 Evolution of the Iceland plume: Os, Nd and He evidence**

340 Initial volcanism, derived from high degree melting, was characterised by approximately chondritic  
341 Os isotope compositions, the highest known  $^3\text{He}/^4\text{He}$  ratios and variable, but fairly radiogenic

342  $^{143}\text{Nd}/^{144}\text{Nd}$  ratios. Osmium isotope compositions are consistent with a depleted, but not ancient  
343 source, with no significant contribution from any enriched component, including the outer core.  
344 Subsequent melts erupted within 1 Myr of the earliest picrites (Ordlingassoq Member) have  
345 elevated  $^{187}\text{Os}/^{188}\text{Os}$  indicating a contribution from enriched material, possibly old recycled crust  
346 plus sediment, which was not tapped in the first phase of plume melting.

347 Osmium and Nd isotope data for Iceland picrites (Brandon et al., 2007) are most easily explained by  
348 a similar recycled crustal component including a small percentage of sediment (~5%), mixed with a  
349 DMM component with higher  $^{143}\text{Nd}/^{144}\text{Nd}$  than the depleted end-member of early NAIP basalts  
350 (Figure 4). High  $^3\text{He}/^4\text{He}$  ratios persist in the Iceland plume (up to 38 Ra in late Tertiary volcanics,  
351 Hilton et al., 1999). Brandon et al. (2007) report elevated  $^{187}\text{Os}$ , but not  $^{186}\text{Os}$ , indicating the  
352 continued lack of core contribution to the Iceland plume source. Intriguingly, Brandon et al. (2007)  
353 found that  $^3\text{He}/^4\text{He}$  increases with  $^{187}\text{Os}/^{188}\text{Os}$  in young Icelandic picrites (Figure 6b), despite the  
354 probable requirement of recycled oceanic crust which would possess very low  $^3\text{He}/^4\text{He}$ . Brandon  
355 and co-authors explained this by two-stage mixing (firstly combining high  $^3\text{He}/^4\text{He}$  mantle and  
356 recycled crust, then mixing with DMM), although the generation of a largely linear array in He-Os  
357 isotope space is difficult to reconcile with the vastly different He concentrations in DMM and a  
358 hybrid recycled crust-high  $^3\text{He}/^4\text{He}$  source, regardless of the ultimate source of the latter.

359

#### 360 **5.4 The $^{187}\text{Os}/^{188}\text{Os}$ composition of convecting mantle**

361 Trace element and Nd-Sr isotope evidence (Stuart et al., 2003; Ellam and Stuart, 2004; Kent et al.,  
362 2004) indicates that the NAP source is typically depleted with respect to putative primitive mantle  
363 (e.g. Zindler and Hart, 1986), and largely indistinguishable from the MORB source mantle (DMM,  
364 e.g. Salters and Stracke, 2004; Workman and Hart, 2005). The  $^{187}\text{Os}/^{188}\text{Os}$  compositions of the  
365 earliest NAP (0.1267 to 0.1280) are consistent with a depleted source containing no significant

366 contribution from recycled crust, pyroxenite, sediment, recycled SCLM, metasomatised peridotite  
367 or outer core, nor any isolated ancient depleted domains. The absence of enriched components in  
368 the source is also supported by the Ni content of picritic olivines. Ni/Mg ratios in the most Mg-rich  
369 olivines ( $Fo > 89$ ) from the Vaigat formation, WG (Larsen and Pedersen, 2000) are lower than those  
370 of other within-plate magmas defined by Sobolev et al. (2007), and also in fact largely lower than  
371 the peridotite range. Although this indicator of pyroxenite contribution has been questioned (see  
372 Niu and O'Hara, 2007), such low Ni/Mg ratios suggest little or no pyroxenite contribution to the  
373 melt. Prytulak and Elliott (2007) proposed that the reference  $TiO_2$  concentration of a OIB suite  
374 (estimated parental melt content, defined as the  $TiO_2$  content on the liquid line of descent typically  
375 at 12.5% MgO), increases with increasing contribution from recycled oceanic crust. The estimated  
376 reference  $TiO_2$  content for the early NAP is  $\leq 1\%$ , lower than all OIB suites compiled by Prytulak  
377 and Elliott (2007) except Iceland, and thus the NAP define the low enriched component end-  
378 member for within plate magmas, i.e. their sources are dominated by peridotite. The reference  $TiO_2$   
379 content for Iceland of  $\sim 1\%$  (Prytulak and Elliott, 2007) seems low compared to many Icelandic  
380 lavas and thus perhaps does not accurately represent the enriched components which have  
381 contributed to recent Icelandic magmas.

382 Due to the large degree of melting during the generation of the NAP, their Os isotope composition  
383 will closely reflect the composition of the bulk mantle source. This, coupled with the chemical  
384 similarity to DMM and absence of enriched components, gives the potential for providing an  
385 estimate of the bulk  $^{187}Os/^{188}Os$  composition of the convecting upper mantle/DMM. To facilitate  
386 comparison with other data such as those for MORB, initial  $^{187}Os/^{188}Os$  for picrites, platinum-group  
387 alloys (PGA) and chromites have been recalculated to the present day by assuming chondritic  
388 evolution of their sources since the time of mantle melting. Strictly speaking the evolution of Os  
389 isotopes since melting may be depressed in relation to chondrite (due to Re depletion) and the true  
390 comparative value will be between the initial and re-corrected values. However, the errors

391 associated with such a correction, given the limited time periods, will be negligible (60 Ma for  
392 NAP, 177 Ma for Tibetan PGA).

393 On the basis of the probability peak for the NAP, the present day  $^{187}\text{Os}/^{188}\text{Os}$  composition of  
394 convecting mantle is estimated to be 0.1276 (Figure 5). This is indistinguishable from the main  
395 PGA peak (0.1276), derived mainly from Tibetan ophiolites (Pearson et al., 2007; Shi et al., 2007).  
396 Recent to Phanerozoic ophiolite-derived chromites define a peak at  $^{187}\text{Os}/^{188}\text{Os} = 0.1283$  and  
397 regression of  $^{187}\text{Os}/^{188}\text{Os}$  versus time gives a mean of 0.1281, which is closer to the NAP value  
398 (Walker et al., 2002b). It is possible that the chromite value could be slightly elevated by  
399 subduction-related enrichment of Re (time-integrated) or radiogenic Os. The  $^{187}\text{Os}/^{188}\text{Os}$  estimate  
400 defined by NAP and PGA is intermediate between averages for carbonaceous, enstatite and  
401 ordinary chondrites (0.1262, 0.1281, 0.1283, respectively, Walker et al., 2002a). It is, however,  
402 significantly lower than the proposed  $^{187}\text{Os}/^{188}\text{Os}$  of 0.1296 for putative primitive upper mantle  
403 (PUM) (Meisel et al., 1996). In addition to the effect of time-integrated depletion of Re through the  
404 generation of continental crust, this difference may arise because many of the peridotites used for  
405 regression by Meisel et al. (2001) have been refertilised and radiogenic Os has been added. The  
406 similarity between the modal NAP Os isotope composition and other estimates of ambient  
407 convecting mantle indicate that a  $^{187}\text{Os}/^{188}\text{Os}$  value somewhere between 0.1275 and 0.1281 might  
408 be an appropriate estimate for ambient convecting mantle from which to calculate Re-Os model  
409 ages for peridotites.

410 Figure 5 here.

411 The least radiogenic MORB ( $^{187}\text{Os}/^{188}\text{Os}$  of 0.1261-0.1272) are isotopically similar to the NAP  
412  $^{187}\text{Os}/^{188}\text{Os}$  peak of 0.1276, but most MORB are significantly more radiogenic with  $^{187}\text{Os}/^{188}\text{Os}$   
413 ratios up to 0.148 (Gannoun et al., 2007). This probably reflects the presence of enriched  
414 components within the DMM and the preferential sampling of these components by the smaller

415 degree melts that constitute MORB, relative to the NAP (e.g. Escrig et al., 2005). If such enriched  
416 components are present in the initial NAP source (which the Nd isotope data suggest), their  
417 signature is insignificant compared to the contribution from depleted peridotite.

418 Walker et al. (2002b) estimated the amount of isolated mafic slab material required in the mantle to  
419 account for the difference (1.2%) between their estimate of the  $^{187}\text{Os}/^{188}\text{Os}$  composition of  
420 convecting upper mantle (0.1281, defined by chromites) and the estimate for PUM (0.1296, Meisel.  
421 Their calculations suggested 1.8% of the entire mantle mass must be isolated slabs for a 1.8 Ga  
422 isolation age and 3.4% for 1 Ga isolation. The difference between convecting mantle and PUM  
423  $^{187}\text{Os}/^{188}\text{Os}$  based on the NAP and Tibetan PGA grains is 1.5% and therefore >2% and ~4% isolated  
424 slab material is required for 1.8 and 1 Ga isolation ages, respectively. However, the probable  
425 extensive Re loss from basaltic oceanic crust during subduction, and the lower Re content of  
426 gabbroic crust (Dale et al., 2007) would lead to greater required inputs, unless the lost Re was  
427 incorporated and isolated in arc/continental crust. These calculations are based on depletion of only  
428 half the total mantle mass, if whole-mantle convection is predominant, estimates could be at least  
429 twice as high. However, as noted above, the likely metasomatic sulphide input to some of the more  
430 radiogenic peridotites used to constrain PUM (Meisel et al., 2001) means that 'primitive' mantle  
431 may not be accurately estimated.

## 432 **5.5 Implications for high $^3\text{He}/^4\text{He}$ in the mantle**

433 Based on the greater compatibility of He than U and Th during mantle melting (Graham et al.,  
434 1990; Parman et al., 2005), it has been proposed that ancient melt depletion will result in reduced  
435 ingrowth of  $^4\text{He}$  and therefore high  $^3\text{He}/^4\text{He}$  in the residue (Class and Goldstein, 2005; Parman,  
436 2007). According to a model matching common  $^3\text{He}/^4\text{He}$  values in oceanic basalts with continental  
437 crust age peaks (Parman, 2007), the source of  $^3\text{He}/^4\text{He}$  up to 50  $R_a$  must have been depleted by  
438 melting and isolated since ~3.7 Ga, or alternatively at least 1 Ga in another model by Class and

439 Goldstein (2005). Depletion of moderately incompatible Re during mantle melting leads, over time,  
440 to  $^{187}\text{Os}/^{188}\text{Os}$  ratios which deviate below the primitive mantle evolution curve. A source depleted  
441 at 3.7 Ga or 1 Ga, and subsequently isolated, should have  $^{187}\text{Os}/^{188}\text{Os}$  of  $\sim 0.102$  or  $\sim 0.122$ ,  
442 respectively. The Os isotope data for NAP are more radiogenic, and are therefore not consistent  
443 with ancient depletion as a source for high  $^3\text{He}/^4\text{He}$ . Even the lowest initial  $^{187}\text{Os}/^{188}\text{Os}$  corresponds  
444 to a Re-depletion model age ( $T_{\text{RD}}$ ) of only  $\sim 0.4$  Ga.  $T_{\text{RD}}$  ages assume that Re is entirely depleted  
445 during melting, and therefore ingrowth of  $^{187}\text{Os}$  ceases after depletion, therefore  $T_{\text{RD}}$  are minimum  
446 ages, but even minor Re depletion as a result of small degree melting would depress  $^{187}\text{Os}/^{188}\text{Os}$   
447 evolution further than observed. For depletion to be the mechanism by which high  $^3\text{He}/^4\text{He}$  are  
448 generated, radiogenic Os, but not He, must have been added subsequently. Sulphide addition could  
449 provide such a mechanism but would likely be accompanied by a flux of other elements.

450 Figure 6 here.

451 The core has also been proposed as a possible source of He enriched in  $^3\text{He}$  (e.g. Macpherson et al.,  
452 1998; Porcelli and Halliday, 2001). The proposed partitioning behaviour of Re and Os (and Pt)  
453 between the inner and outer core has led to the hypothesis that the outer core will possess supra-  
454 chondritic Re/Os ratios (and Pt/Os, e.g. Brandon et al., 1998). Therefore, the approximately  
455 chondritic  $^{187}\text{Os}/^{188}\text{Os}$  of extremely high  $^3\text{He}/^4\text{He}$  picrites studied here precludes a bulk contribution  
456 from core material. However, decoupling of core-mantle transfer of Os and He could result in high  
457  $^3\text{He}/^4\text{He}$  without correspondingly high  $^{187}\text{Os}/^{188}\text{Os}$ .

458 The high  $^3\text{He}/^4\text{He}$  component cannot be linked to mantle with a specific Os isotope signature,  
459 because  $^3\text{He}/^4\text{He}$  ratios up to 48 are found in picrites with  $^{187}\text{Os}/^{188}\text{Os}$  of  $\sim 0.1267$  to  $0.132$ .  
460 However, if the elevated  $^{187}\text{Os}/^{188}\text{Os}$  can be explained by a minor recycled crust component (small  
461 enough not to overwrite the high  $^3\text{He}/^4\text{He}$  signature, c.f. Macpherson et al. (2005) for Iceland), or  
462 metasomatic sulphide transfer from such sources, then the end-member high  $^3\text{He}/^4\text{He}$  component

463 would have a  $^{187}\text{Os}/^{188}\text{Os}$  of  $\sim 0.1276$  – defined by the NAP, indistinguishable from the main PGA  
464 peak and similar to the least radiogenic MORB. It is not possible to conclude, from these data, the  
465 ultimate source of the high  $^3\text{He}/^4\text{He}$  signature that was tapped most efficiently during melting of the  
466 plume-head and persists in Icelandic volcanism today. However, it is possible that He is decoupled  
467 from Os and Nd and could reflect a ‘primitive’ component which is volumetrically small, hence not  
468 changing Os or Nd isotopes significantly, but rich enough in He to strongly affect the  $^3\text{He}/^4\text{He}$  ratio.  
469 Alternatively, although the mechanisms are not well understood, it has been proposed that a high  
470  $^3\text{He}/^4\text{He}$  component could be present in some upper mantle material (e.g. Meibom et al., 2003),  
471 although, if so, such material must only be sampled during episodes of large degree melting of hot  
472 mantle.

## 473 **6. Concluding remarks**

474 Osmium concentrations in NAP are very high (up to 4.02 ng/g, mean: 2.15 ng/g) and suggest  
475 complete consumption of sulphide in at least part of the source due to large degree melting ( $\geq 20\%$   
476 for a fertile source). This is consistent with previous evaluations of the degree of melting based on  
477 MgO-rich olivines: 10-11% for depleted mantle,  $>20\text{-}28\%$  for fertile mantle (Herzberg and O'Hara,  
478 2002). Initial Os isotope compositions in the earliest picritic melts from West Greenland (Anaanaa  
479 and Naujánguit Members of the Vaigat formation) and Baffin Island are uniform and broadly  
480 chondritic (probability peak of  $^{187}\text{Os}/^{188}\text{Os} = 0.1272$ ). This initial volcanism cannot contain any  
481 significant contribution from the outer core or from old recycled crustal material, as both would  
482 impart a radiogenic  $^{187}\text{Os}/^{188}\text{Os}$  signature. In addition, minimal presence of enriched pyroxenitic  
483 components in the source of NAP is suggested by various parameters such as Ni content of olivine  
484 and  $\text{TiO}_2$  content. The absence of enriched components, coupled with a large degree of melting,  
485 means that the average  $^{187}\text{Os}/^{188}\text{Os}$  (corrected to 0.1276 for the present day) may reflect the bulk  
486  $^{187}\text{Os}/^{188}\text{Os}$  of convecting mantle. This value is similar to the least radiogenic MORB (e.g.

487 Gannoun et al., 2007) and the most common  $^{187}\text{Os}/^{188}\text{Os}$  ratios found in PGA grains from Tibetan  
488 ophiolites (Pearson et al., 2007; Shi et al., 2007). Subsequent melts sampled from the Ordlingassoq  
489 Member (upper Vaigat formation), erupted within 1 Myr of the earliest melts (Storey et al., 1998),  
490 possess supra-chondritic initial  $^{187}\text{Os}/^{188}\text{Os}$  ratios of up to 0.1321, which can be accounted for  
491 (though not exclusively) by a greater contribution from recycled crust. These more enriched  
492 signatures are seen in more recent melts from the Iceland plume (Brandon et al., 2007).

493 Models seeking to explain high  $^3\text{He}/^4\text{He}$  ratios by ancient depletion (Class and Goldstein, 2005;  
494 Parman, 2007) are not supported by the uniform and largely chondritic  $^{187}\text{Os}/^{188}\text{Os}$  ratios of NAP  
495 which possess the highest known mantle-derived  $^3\text{He}/^4\text{He}$  ratios (up to 50 Ra, Stuart et al., 2003). If  
496 ancient melting and isolation had occurred, the depletion of Re during melting would lead to  
497 significantly sub-chondritic  $^{187}\text{Os}/^{188}\text{Os}$  in the depleted source ( $\sim 0.122$  and  $\sim 0.102$  for depletion  
498 ages of 1 Ga and 3.7 Ga, Class and Goldstein (2005), and Parman (2007) models respectively).  
499 Conversely, outer core material would impart radiogenic Os to the plume and so core material is  
500 also not supported as a source of high  $^3\text{He}/^4\text{He}$  unless the mechanism of He transfer to the plume is  
501 decoupled from Os. High  $^3\text{He}/^4\text{He}$  mantle is not otherwise isotopically distinct from a typical upper  
502 mantle source, in terms of Os or other radiogenic isotopes. Therefore two possible explanations for  
503 the high  $^3\text{He}/^4\text{He}$  signature are: (i) it is present in a typical upper mantle source which has been  
504 entrained in the plume-head, but is only tapped during episodes of high-degree melting of hot  
505 mantle; (ii) the He isotope signature is entirely decoupled from other elements and is dominated by  
506 addition of a He-rich, high  $^3\text{He}/^4\text{He}$  component, probably primordial in nature, without  
507 complementary addition of other elements. The latter is our favoured model.

508 **Acknowledgements**

509 C. Dale thanks the Natural Environment Research Council (NERC) for supporting this work as part  
510 of standard grant, NE/C51902x/1. We are grateful to Sarah Woodland for some Os isotope  
511 analyses and to Chris Ottley for assistance with Re measurements.

512 main text: ~6330

513 **References**

- 514 Ballhaus, C., Bockrath, C., Wohlgemuth-Ueberwasser, C., Laurenz, V. and Berndt, J., 2006.  
515 Fractionation of the noble metals by physical processes. *Contributions to Mineralogy and*  
516 *Petrology*, 152(6): 667-684.
- 517 Becker, H., Horan, M.F., Walker, R.J. et al., 2006. Highly siderophile element composition of the  
518 Earth's primitive upper mantle: Constraints from new data on peridotite massifs and  
519 xenoliths. *Geochimica Et Cosmochimica Acta*, 70(17): 4528-4550.
- 520 Bennett, V.C., Esat, T.M. and Norman, M.D., 1996. Two mantle-plume components in Hawaiian  
521 picrites inferred from correlated Os-Pb isotopes. *Nature*, 381(6579): 221-224.
- 522 Brandon, A.D., Walker, R.J., Morgan, J.W., Norman, M.D. and Prichard, H.M., 1998. Coupled  
523  $^{186}\text{Os}$  and  $^{187}\text{Os}$  evidence for core-mantle interaction. *Science*, 280(5369): 1570-1573.
- 524 Brandon, A.D., Norman, M.D., Walker, R.J. and Morgan, J.W., 1999.  $^{186}\text{Os}$ - $^{187}\text{Os}$  systematics of  
525 Hawaiian picrites. *Earth and Planetary Science Letters*, 174(1-2): 25-42.
- 526 Brandon, A.D., Snow, J.E., Walker, R.J., Morgan, J.W. and Mock, T.D., 2000.  $^{190}\text{Pt}$ - $^{186}\text{Os}$  and  
527  $^{187}\text{Re}$ - $^{187}\text{Os}$  systematics of abyssal peridotites. *Earth and Planetary Science Letters*, 177(3-  
528 4): 319-335.
- 529 Brandon, A.D., Graham, D.W., Waight, T. and Gautason, B., 2007.  $^{186}\text{Os}$  and  $^{187}\text{Os}$  enrichments  
530 and high- $^3\text{He}/^4\text{He}$  sources in the Earth's mantle: Evidence from Icelandic picrites.  
531 *Geochimica et Cosmochimica Acta*, 71(18): 4570-4591.
- 532 Burton, K.W., Gannoun, A., Birck, J.-L. et al., 2002. The compatibility of rhenium and osmium in  
533 natural olivine and their behaviour during mantle melting and basalt genesis. *Earth and*  
534 *Planetary Science Letters*, 198(1-2): 63-76.
- 535 Class, C. and Goldstein, S.L., 2005. Evolution of helium isotopes in the Earth's mantle. *Nature*,  
536 436(7054): 1107-1112.
- 537 Cohen, A.S. and Waters, F.G., 1996. Separation of osmium from geological materials by solvent  
538 extraction for analysis by thermal ionisation mass spectrometry. *Analytica Chimica Acta*,  
539 332(2-3): 269-275.
- 540 Crocket, J.H., Fleet, M.E. and Stone, W.E., 1997. Implications of composition for experimental  
541 partitioning of platinum-group elements and gold between sulfide liquid and basalt melt:  
542 The significance of nickel content. *Geochimica Et Cosmochimica Acta*, 61(19): 4139-4149.
- 543 Dale, C.W., Gannoun, A., Burton, K.W., Argles, T.W. and Parkinson, I.J., 2007. Rhenium–osmium  
544 isotope and elemental behaviour during subduction of oceanic crust and the implications for  
545 mantle recycling. *Earth and Planetary Science Letters*, 253: 211-225.

- 546 Dale, C.W., Luguet, A., Macpherson, C.G., Pearson, D.G. and Hickey-Vargas, R., 2008. Extreme  
547 platinum-group element fractionation and variable Os isotope compositions in Philippine  
548 Sea Plate basalts: Tracing mantle source heterogeneity. *Chemical Geology*, 248(3-4): 213-  
549 238.
- 550 Ellam, R.M. and Stuart, F.M., 2004. Coherent He-Nd-Sr isotope trends in high He-3/He-4 basalts:  
551 implications for a common reservoir, mantle heterogeneity and convection. *Earth and*  
552 *Planetary Science Letters*, 228(3-4): 511-523.
- 553 Escrig, S., Schiano, P., Schilling, J.G. and Allegre, C., 2005. Rhenium-osmium isotope systematics  
554 in MORB from the Southern Mid-Atlantic Ridge (40 degrees-50 degrees S). *Earth and*  
555 *Planetary Science Letters*, 235(3-4): 528-548.
- 556 Esser, B.K. and Turekian, K.K., 1993. The osmium isotopic composition of the continental crust.  
557 *Geochimica et Cosmochimica Acta*, 57(13): 3093-3104.
- 558 Francis, D., 1985. The Baffin-Bay Lavas and the Value of Picrites as Analogs of Primary Magmas.  
559 *Contributions to Mineralogy and Petrology*, 89(2-3): 144-154.
- 560 Gannoun, A., Burton, K.W., Parkinson, I.J. et al., 2007. The scale and origin of the osmium isotope  
561 variations in mid-ocean ridge basalts. *Earth and Planetary Science Letters*, 259(3-4): 541-  
562 556.
- 563 Gill, R.C.O., Pedersen, A.K. and Larsen, J.G., 1992. Tertiary picrites in West Greenland: melting at  
564 the periphery of a plume? In: B.C. Storey, T. Alabaster and R.J. Pankhurst (Editors),  
565 *Magmatism and the causes of continental break-up*. Geol. Soc. London, Spec. Publ.
- 566 Graham, D., Lupton, J., Albarede, F. and Condomines, M., 1990. Extreme Temporal Homogeneity  
567 of Helium-Isotopes at Piton-De-La-Fournaise, Reunion Island. *Nature*, 347(6293): 545-548.
- 568 Graham, D.W., Larsen, L.M., Hanan, B.B. et al., 1998. Helium isotope composition of the early  
569 Iceland mantle plume inferred from the tertiary picrites of West Greenland. *Earth and*  
570 *Planetary Science Letters*, 160(3-4): 241-255.
- 571 Graham, D.W., 2003. Noble Gas Isotope Geochemistry of Mid-Ocean Ridge and Ocean Island  
572 Basalts: Characterization of Mantle Source Reservoirs. In: D. P. Porcelli, C.J. Ballentine and  
573 R. Wieler (Editors), *Noble Gases. Reviews in Mineralogy and Geochemistry*, 47.
- 574 Harvey, J., Gannoun, A., Burton, K.W. et al., 2006. Ancient melt extraction from the oceanic upper  
575 mantle revealed by Re-Os isotopes in abyssal peridotites from the Mid-Atlantic ridge. *Earth*  
576 *and Planetary Science Letters*, 244(3-4): 606-621.
- 577 Hauri, E.H. and Hart, S.R., 1993. Re-Os Isotope Systematics of HIMU and EM-II Oceanic Island  
578 Basalts from the South-Pacific Ocean. *Earth and Planetary Science Letters*, 114(2-3): 353-  
579 371.

- 580 Hauri, E.H., Lassiter, J.C. and DePaolo, D.J., 1996. Osmium isotope systematics of drilled lavas  
581 from Mauna Loa, Hawaii. *Journal of Geophysical Research-Solid Earth*, 101(B5): 11793-  
582 11806.
- 583 Herzberg, C. and O'Hara, M.J., 2002. Plume-associated ultramafic magmas of Phanerozoic age.  
584 *Journal of Petrology*, 43(10): 1857-1883.
- 585 Hilton, D.R., Gronvold, K., Macpherson, C.G. and Castillo, P.R., 1999. Extreme  $^3\text{He}/^4\text{He}$  ratios in  
586 northwest Iceland: constraining the common component in mantle plumes. *Earth and*  
587 *Planetary Science Letters*, 173(1-2): 53-60.
- 588 Holm, P.M., Gill, R.C.O., Pedersen, A.K. et al., 1993. The Tertiary Picrites of West Greenland -  
589 Contributions from Icelandic and Other Sources. *Earth and Planetary Science Letters*,  
590 115(1-4): 227-244.
- 591 Kent, A.J.R., Stolper, E.M., Francis, D. et al., 2004. Mantle heterogeneity during the formation of  
592 the North Atlantic Igneous Province: Constraints from trace element and Sr-Nd-Os-O  
593 isotope systematics of Baffin Island picrites. *Geochemistry Geophysics Geosystems*, 5.
- 594 Kurz, M.D., Jenkins, W.J. and Hart, S.R., 1982. Helium Isotopic Systematics of Oceanic Islands  
595 and Mantle Heterogeneity. *Nature*, 297(5861): 43-47.
- 596 Larsen, L.M. and Pedersen, A.K., 2000. Processes in high-mg, high-T magmas: Evidence from  
597 olivine, chromite and glass in Palaeogene picrites from West Greenland. *Journal of*  
598 *Petrology*, 41(7): 1071-1098.
- 599 Lightfoot, P.C., Hawkesworth, C.J., Olshefsky, K. et al., 1997. Geochemistry of tertiary tholeiites  
600 and picrites from Qeqertarsuaq (Disko Island) and Nuussuaq, West Greenland with  
601 implications for the mineral potential of comagmatic intrusions. *Contributions to*  
602 *Mineralogy and Petrology*, 128(2-3): 139-163.
- 603 Lorand, J.P., Alard, O., Luguet, A. and Keays, R.R., 2003. Sulfur and selenium systematics of the  
604 subcontinental lithospheric mantle: Inferences from the Massif Central xenolith suite  
605 (France). *Geochimica Et Cosmochimica Acta*, 67(21): 4137-4151.
- 606 Luguet, A., Nowell, G.M. and Pearson, D.G., 2008.  $^{184}\text{Os}/^{188}\text{Os}$  and  $^{186}\text{Os}/^{188}\text{Os}$  measurements by  
607 Negative Thermal Ionisation Mass Spectrometry (N-TIMS): Effects of interfering element  
608 and mass fractionation corrections on data accuracy and precision. *Chemical Geology*,  
609 248(3-4): 342-362.
- 610 Macpherson, C.G., Hilton, D.R., Sinton, J.M., Poreda, R.J. and Craig, H., 1998. High  $^3\text{He}/^4\text{He}$  ratios  
611 in the Manus backarc basin: Implications for mantle mixing and the origin of plumes in the  
612 western Pacific Ocean. *Geology*, 26(11): 1007-1010.
- 613 Macpherson, C.G., Hilton, D.R., Day, J.M.D., Lowry, D. and Gronvold, K., 2005. High- $^3\text{He}/^4\text{He}$ ,  
614 depleted mantle and low- $\delta\text{O-18}$ , recycled oceanic lithosphere in the source of central  
615 Iceland magmatism. *Earth and Planetary Science Letters*, 233(3-4): 411-427.

- 616 Marcantonio, F., Zindler, A., Elliott, T. and Staudigel, H., 1995. Os Isotope Systematics of La  
617 Palma, Canary-Islands - Evidence for Recycled Crust in the Mantle Source of HIMU Ocean  
618 Islands. *Earth and Planetary Science Letters*, 133(3-4): 397-410.
- 619 Martin, C.E., 1991. Osmium Isotopic Characteristics of Mantle-Derived Rocks. *Geochimica et*  
620 *Cosmochimica Acta*, 55(5): 1421-1434.
- 621 Martin, C.E., Carlson, R.W., Shirey, S.B., Frey, F.A. and Chen, C.Y., 1994. Os-Isotopic Variation  
622 in Basalts from Haleakala Volcano, Maui, Hawaii - a Record of Magmatic Processes in  
623 Oceanic Mantle and Crust. *Earth and Planetary Science Letters*, 128(3-4): 287-301.
- 624 Mavrogenes, J.A. and O'Neill, H.S.C., 1999. The relative effects of pressure, temperature and  
625 oxygen fugacity on the solubility of sulfide in mafic magmas. *Geochimica Et Cosmochimica*  
626 *Acta*, 63(7-8): 1173-1180.
- 627 Meibom, A., Sleep, N.H., Chamberlain, C.P. et al., 2002. Re-Os isotopic evidence for long-lived  
628 heterogeneity and equilibration processes in the Earth's upper mantle. *Nature*, 419(6908):  
629 705-708.
- 630 Meibom, A., Anderson, D.L., Sleep, N.H. et al., 2003. Are high  $^3\text{He}/^4\text{He}$  ratios in oceanic basalts an  
631 indicator of deep-mantle plume components? *Earth and Planetary Science Letters*, 208(3-4):  
632 197-204.
- 633 Meisel, T., Walker, R.J. and Morgan, J.W., 1996. The osmium isotopic composition of the Earth's  
634 primitive upper mantle. *Nature*, 383(6600): 517-520.
- 635 Meisel, T., Walker, R.J., Irving, A.J. and Lorand, J.P., 2001. Osmium isotopic compositions of  
636 mantle xenoliths: A global perspective. *Geochimica Et Cosmochimica Acta*, 65(8): 1311-  
637 1323.
- 638 Moreira, M., Breddam, K., Curtice, J. and Kurz, M.D., 2001. Solar neon in the Icelandic mantle:  
639 new evidence for an undegassed lower mantle. *Earth and Planetary Science Letters*, 185(1-  
640 2): 15-23.
- 641 Morgan, J.W., Walker, R.J., Brandon, A.D. and Horan, M.F., 2001. Siderophile elements in Earth's  
642 upper mantle and lunar breccias: Data synthesis suggests manifestations of the same late  
643 influx. *Meteoritics & Planetary Science*, 36(9): 1257-1275.
- 644 Niu, Y.L. and O'Hara, M.J., 2003. Origin of ocean island basalts: A new perspective from  
645 petrology, geochemistry, and mineral physics considerations. *Journal of Geophysical*  
646 *Research-Solid Earth*, 108(B4).
- 647 Niu, Y.L. and O'Hara, M.J., 2007. Varying Ni in OIB olivines - Product of process not source.  
648 *Geochimica et Cosmochimica Acta*, 71(15): A721.
- 649 Parman, S.W., Kurz, M.D., Hart, S.R. and Grove, T.L., 2005. Helium solubility in olivine and  
650 implications for high  $\text{He-3}/\text{He-4}$  in ocean island basalts. *Nature*, 437(7062): 1140-1143.

- 651 Parman, S.W., 2007. Helium isotopic evidence for episodic mantle melting and crustal growth.  
652 Nature, 446(7138): 900-903.
- 653 Pearson, D.G. and Woodland, S.J., 2000. Solvent extraction/anion exchange separation and  
654 determination of PGEs (Os, Ir, Pt, Pd, Ru) and Re-Os isotopes in geological samples by  
655 isotope dilution ICP-MS. *Chemical Geology*, 165(1-2): 87-107.
- 656 Pearson, D.G., Parman, S.W. and Nowell, G.M., 2007. A link between large mantle melting events  
657 and continent growth seen in osmium isotopes. *Nature*, 449(7159): 202-205.
- 658 Pedersen, A.K., 1985. Reaction between picrite magma and continental crust: early Tertiary silicic  
659 basalts and magnesian andesites from Disko, West Greenland. *Bulletin Grønlands*  
660 *Geologiske Undersøgelse*, 152: 126 pp.
- 661 Pedersen, A.K., Larsen, L.M., Riisager, P. and Dueholm, K.S., 2002. Rates of volcanic deposition,  
662 facies changes and movements in a dynamic basin: the Nuussuaq Basin, West Greenland,  
663 around the C27n-C26r transition. . In: D.W. Jolley and B.R. Bell (Editors), *The North*  
664 *Atlantic Igneous Province: stratigraphy, tectonics, volcanic and magmatic processes.*  
665 *Geological Society, London*, 197, pp. 157-181.
- 666 Peucker-Ehrenbrink, B. and Jahn, B.M., 2001. Rhenium-osmium isotope systematics and platinum  
667 group element concentrations: Loess and the upper continental crust. *Geochemistry*  
668 *Geophysics Geosystems*, 2: art. no.-2001GC000172.
- 669 Porcelli, D. and Halliday, A.N., 2001. The core as a possible source of mantle helium. *Earth and*  
670 *Planetary Science Letters*, 192(1): 45-56.
- 671 Porcelli, D., Ballentine, C.J. and Wieler, R., 2002. An overview of noble gas - Geochemistry and  
672 cosmochemistry. *Noble Gases in Geochemistry and Cosmochemistry*, 47: 1-19.
- 673 Prytulak, J. and Elliott, T., 2007. TiO<sub>2</sub> enrichment in ocean island basalts. *Earth and Planetary*  
674 *Science Letters*, 263(3-4): 388-403.
- 675 Reisberg, L., Zindler, A., Marcantonio, F. et al., 1993. Os Isotope Systematics in Ocean Island  
676 Basalts. *Earth and Planetary Science Letters*, 120(3-4): 149-167.
- 677 Robillard, I., Francis, D. and Ludden, J.N., 1992. The Relationship between E-Type and N-Type  
678 Magmas in the Baffin-Bay Lavas. *Contributions to Mineralogy and Petrology*, 112(2-3):  
679 230-241.
- 680 Roy-Barman, M. and Allegre, C.J., 1994. <sup>187</sup>Os-<sup>186</sup>Os Ratios of Midocean Ridge Basalts and  
681 Abyssal Peridotites. *Geochimica et Cosmochimica Acta*, 58(22): 5043-5054.
- 682 Salters, V.J.M. and Stracke, A., 2004. Composition of the depleted mantle. *Geochemistry*  
683 *Geophysics Geosystems*, 5: art. no.-Q05004.

- 684 Saunders, A.D., Fitton, J.G., Kerr, A.C., Norry, M.J. and Kent, R.W., 1997. The North Atlantic  
685 Igneous Province. In: J.J. Mahoney and M.F. Coffin (Editors), Large Igneous Provinces.  
686 Geophysical monograph. Vol. 100, pp. 45-94.
- 687 Schaefer, B.F., Parkinson, I.J. and Hawkesworth, C.J., 2000. Deep mantle plume osmium isotope  
688 signature from West Greenland Tertiary picrites. *Earth and Planetary Science Letters*,  
689 175(1-2): 105-118.
- 690 Schiano, P., Birck, J.L. and Allegre, C.J., 1997. Osmium-strontium-neodymium-lead isotopic  
691 covariations in mid-ocean ridge basalt glasses and the heterogeneity of the upper mantle.  
692 *Earth and Planetary Science Letters*, 150(3-4): 363-379.
- 693 Shi, R.D., Alard, O., Zhi, X.C. et al., 2007. Multiple events in the Neo-Tethyan oceanic upper  
694 mantle: Evidence from Ru-Os-Ir alloys in the Luobusa and Dongqiao ophiolitic podiform  
695 chromitites, Tibet. *Earth and Planetary Science Letters*, 261(1-2): 33-48.
- 696 Snow, J.E. and Reisberg, L., 1995. Os isotopic systematics of the MORB mantle: results from  
697 altered abyssal peridotites. *Earth and Planetary Science Letters*, 133(3-4): 411-421.
- 698 Sobolev, A.V., Hofmann, A.W., Kuzmin, D.V. et al., 2007. The amount of recycled crust in sources  
699 of mantle-derived melts. *Science*, 316(5823): 412-417.
- 700 Starkey, N., Stuart, F.M., Ellam, R.M. et al., 2007. No role for discrete, depleted high  $^3\text{He}/^4\text{He}$   
701 mantle. *Geochimica et Cosmochimica Acta*, 71(15): A967.
- 702 Storey, M., Duncan, R.A., Pedersen, A.K., Larsen, L.M. and Larsen, H.C., 1998.  $^{40}\text{Ar}/^{39}\text{Ar}$   
703 geochronology of the West Greenland Tertiary volcanic province. *Earth and Planetary*  
704 *Science Letters*, 160(3-4): 569-586.
- 705 Stracke, A., Bizimis, M. and Salters, V.J.M., 2003. Recycling oceanic crust: Quantitative  
706 constraints. *Geochemistry Geophysics Geosystems*, 4: art. no.-8003.
- 707 Stuart, F.M., Lass-Evans, S., Fitton, J.G. and Ellam, R.M., 2003. High  $^3\text{He}/^4\text{He}$  ratios in picritic  
708 basalts from Baffin Island and the role of a mixed reservoir in mantle plumes. *Nature*,  
709 424(6944): 57-59.
- 710 Sun, W., Bennett, V.C., Eggins, S.M., Arculus, R.J. and Perfit, M.R., 2003. Rhenium systematics in  
711 submarine MORB and back-arc basin glasses: laser ablation ICP-MS results. *Chemical*  
712 *Geology*, 196(1-4): 259-281.
- 713 Taylor, R.N., Thirlwall, M.F., Murton, B.J., Hilton, D.R. and Gee, M.A.M., 1997. Isotopic  
714 constraints on the influence of the Icelandic plume. *Earth and Planetary Science Letters*,  
715 148(1-2): E1-E8.
- 716 Theriault, R.J., St-Onge, M.R. and Scott, D.J., 2001. Nd isotopic and geochemical signature of the  
717 paleoproterozoic Trans-Hudson Orogen, southern Baffin Island, Canada: implications for  
718 the evolution of eastern Laurentia. *Precambrian Research*, 108(1-2): 113-138.

- 719 Thirlwall, M.F., Gee, M.A.M., Taylor, R.N. and Murton, B.J., 2004. Mantle components in Iceland  
720 and adjacent ridges investigated using double-spike Pb isotope ratios. *Geochimica Et*  
721 *Cosmochimica Acta*, 68(2): 361-386.
- 722 Thompson, R.N., Gibson, S.A., Dickin, A.P. and Smith, P.M., 2001. Early Cretaceous basalt and  
723 picrite dykes of the southern Etendeka region, NW Namibia: Windows into the role of the  
724 Tristan mantle plume in Parana-Etendeka magmatism. *Journal of Petrology*, 42(11): 2049-  
725 2081.
- 726 Walker, R.J., Horan, M.F., Morgan, J.W. et al., 2002a. Comparative Re-187-Os-187 systematics of  
727 chondrites: Implications regarding early solar system processes. *Geochimica et*  
728 *Cosmochimica Acta*, 66(23): 4187-4201.
- 729 Walker, R.J., Prichard, H.M., Ishiwatari, A. and Pimentel, M., 2002b. The osmium isotopic  
730 composition of convecting upper mantle deduced from ophiolite chromites. *Geochimica et*  
731 *Cosmochimica Acta*, 66(2): 329-345.
- 732 Widom, E. and Shirey, S.B., 1996. Os isotope systematics in the Azores: Implications for mantle  
733 plume sources. *Earth and Planetary Science Letters*, 142(3-4): 451-465.
- 734 Widom, E., Hoernle, K.A., Shirey, S.B. and Schmincke, H.U., 1999. Os isotope systematics in the  
735 Canary Islands and Madeira: Lithospheric contamination and mantle plume signatures.  
736 *Journal of Petrology*, 40(2): 279-296.
- 737 Workman, R.K. and Hart, S.R., 2005. Major and trace element composition of the depleted MORB  
738 mantle (DMM). *Earth and Planetary Science Letters*, 231(1-2): 53-72.
- 739 Zindler, A. and Hart, S., 1986. Chemical Geodynamics. *Annual Review of Earth and Planetary*  
740 *Sciences*, 14: 493-571.  
741  
742

743 **Figure captions**

744

745 Figure 1. Co-variation of Os and Re with MgO in West Greenland, Baffin Island and Iceland  
746 picrites. Icelandic picrite data from Brandon et al. (2007).

747

748

749 Figure 2. Probability density plot for initial  $^{187}\text{Os}/^{188}\text{Os}$  in (a) Baffin Island & West Greenland  
750 picrites (NAP) from this study and (b) NAP and Iceland picrites from the literature. Other data: <sup>1</sup>  
751 Schaefer et al. (2000), <sup>2</sup> Brandon et al. (2007), <sup>3</sup> Kent et al. (2004). NAP samples with <0.5 ng/g Os  
752 have been omitted due to potential crustal contamination. A ‘bandwidth’ uncertainty of 0.001 was  
753 applied to the  $^{187}\text{Os}/^{188}\text{Os}$  ratio of all samples (~0.8% relative uncertainty).

754

755 Figure 3. Initial  $^{187}\text{Os}/^{188}\text{Os}$  (at 61 Ma) plotted against Os concentration. PI, DI and CS are  
756 Padloping Island, Durban Island and Cape Searle. An, Nau and Ord are, oldest to youngest,  
757 Anaanaa, Naujánguit and Ordlingassoq Members of the Vaigat formation. A lack of co-variation  
758 suggests insignificant assimilation of radiogenic ancient crust and/or unradiogenic SCLM. Only the  
759 duplicated low Os CS sample has slightly more radiogenic Os than others from Baffin Island,  
760 consistent with a minor crustal contribution. Primitive mantle estimate (without uncertainty) from  
761 Meisel et al. (2001), abyssal peridotites (AP) from Snow and Reisberg (1995) and Harvey et al.  
762 (2006), carbonaceous chondrite (without uncertainty) from Walker et al. (2002a). Other WG data  
763 from Schaefer et al. (2000), other BI data from Kent et al. (2004), Hawaii and Iceland data from  
764 Brandon et al. (1999; 2007, respectively).

765

766 Figure 4. (a)  $^{187}\text{Os}/^{188}\text{Os}$  vs.  $^{143}\text{Nd}/^{144}\text{Nd}$  (both age corrected to 61 Ma), for NAP in this study and  
767 NAP and Iceland picrites from the literature (Schaefer et al., 2000; Kent et al., 2004; Brandon et al.,  
768 2007, respectively). (b) Assessment of mixing enriched materials with mantle. Crustal  
769 contamination: black lines – best estimate/average, (Sm-Nd data from Larsen (unpubl.) - thick, and  
770 Theriault et al. (2001) - thin), grey area – whole possible range. Enriched plume components in the  
771 source: thick green line – 2 Ga oceanic crust with 5-10% sediment, thin green line - 2Ga oceanic  
772 crust. Literature data sources - see Figure 3, except DMM Nd estimate from Workman and Hart  
773 (2005) and Salters and Stracke (2004). Mixing lines calculated using 2 Ga recycled crust Nd  
774 isotope composition estimates from Stracke et al. (2003) and Os compositions calculated from  
775 Schiano (1997), Gannoun et al. (2007) and Dale et al. (2007). Crustal Os compositions based on  
776 average continental crust (Peucker-Ehrenbrink and Jahn, 2001) and Os data for granites (Dale,  
777 unpubl.). Lighter depleted mantle ornament denotes likely end-member for Iceland array.

778

779 Figure 5. Probability density plot for  $^{187}\text{Os}/^{188}\text{Os}$  of NAP (this study and literature) and other direct  
780 and indirect indicators of mantle composition.  $^{187}\text{Os}/^{188}\text{Os}$  of the picrites has been corrected for  
781 ingrowth since emplacement, but then recalculated to a present day composition (by means of  
782 deviation from chondrite evolution curve). Data for chromites<sup>3</sup> (Walker et al., 2002b) are also  
783 corrected to present day (\* mean value for chromites taken from the authors' regression using  
784  $^{187}\text{Os}/^{188}\text{Os}$  vs. time, not the peak on this plot). Other data sources: <sup>1</sup> Schaefer et al. (2000) and  
785 Kent et al. (2004), <sup>2</sup> Pearson et al. (2007) and Shi et al. (2007), <sup>4</sup> Roy-Barman and Allegre (1994),  
786 Snow and Reisberg (1995), Brandon et al. (2000) and Harvey et al. (2006), <sup>5</sup> Gannoun et al. (2007),  
787 Global OIB data from samples with >30 pg/g Os from: Martin, (1991), Hauri and Hart (1993),  
788 Reisberg et al. (1993), Martin et al. (1994), Marcantonio et al. (1995), Bennett et al. (1996), Hauri  
789 et al. (1996), Widom and Shirey (1996), Widom et al. (1999). EC, OC and CC are enstatite,  
790 ordinary and carbonaceous chondrites, respectively (Walker et al., 2002a), PUM is primitive upper

791 mantle (Meisel et al., 2001). NAP with <0.5 ng/g Os have been omitted due to potential crustal  
792 contamination. A ‘bandwidth’ uncertainty of 0.001 was applied to the  $^{187}\text{Os}/^{188}\text{Os}$  ratio of all  
793 samples (~0.8% relative uncertainty).

794

795 Figure 6. (a) He isotope composition against  $^{187}\text{Os}/^{188}\text{Os}$  at the time of eruption (61 Ma) for picrites  
796 in this study, and (b) probability density plot for  $^{187}\text{Os}/^{188}\text{Os}$  ratios (not corrected to present day) in  
797 picrites from this study, Icelandic picrites (Brandon et al., 2007), global ocean island basalts and  
798 picrites, and platinum-group alloys (PGA) from ophiolites in Tasmania, Tibet and the Urals  
799 (Pearson et al., 2007). (b) Symbols: see Figure 1. Mantle ages refer to the time of melt depletion.  
800 He compositions for these ages are based on: <sup>1</sup> Class and Goldstein (2005), <sup>2</sup> Parman et al. (2007).  
801 Helium isotope data from Stuart et al. (2003), Starkey et al. (2007) and Starkey et al. (in review).  
802 Also shown are picrites from Hawaii (Brandon et al., 1999).

Table 1

[Click here to download Table: Table 1 a.doc](#)

Table 1. Re-Os isotope and elemental data for North Atlantic picrites (NAP, Baffin Island and Vaigat formation, West Greenland).

	Dig. method	Os ng/g	Re ng/g	Re/Os	<sup>187</sup> Os/ <sup>188</sup> Os	<sup>187</sup> Os/ <sup>188</sup> Os <sub>i</sub>	<sup>187</sup> Re/ <sup>188</sup> Os	γOs	MgO wt. %	Ni μg/g	Yb μg/g
<b>Baffin Island</b>											
<i>Padloping Island</i>											
PI-23	CT	1.477	-	-	0.12849	-	-	-	24.51	1127	1.28
PI-24	HPA	1.827	0.173	0.095	0.12775	0.12729	0.457	0.10	26.10	1228	1.27
PI-25	HPA	2.555	0.101	0.040	0.12780	0.12761	0.191	0.35	27.69	1336	1.01
PI-26	HPA	2.028	0.251	0.124	0.12758	0.12698	0.596	-0.15	25.09	1190	1.24
dupl.	HPA	1.927	0.253	0.131	0.12775	0.12711	0.631	-0.04	25.09	1190	1.24
dupl.	CT	1.974	-	-	0.12760	-	-	-	25.09	1190	1.24
PI-27	HPA	1.369	0.336	0.245	0.12896	0.12775	1.168	0.46	23.20	1058	1.30
dupl.	CT	1.483	-	-	0.12849	-	-	-	23.20	1058	1.30
PI-31	HPA	1.762	0.294	0.167	0.12816	0.12734	0.803	0.14	22.64	1027	1.48
PI-37	HPA	3.445	0.120	0.035	0.12692	0.12675	0.168	-0.33	26.57	1206	1.07
PI-43	HPA	2.106	0.295	0.140	0.12777	0.12708	0.674	-0.06	24.58	1081	1.37
PAD-6	HPA	1.084	0.419	0.387	0.12878	0.12689	1.86	-1.06	17.20	647	1.70
<i>Durban Island</i>											
DI-23	CT	2.549	0.097	0.038	0.12751	0.12732	0.182	0.12	24.14	1035	1.32
DI-26	HPA	0.909	0.286	0.315	0.12855	0.12701	1.52	-0.11	15.92	546	1.70
DUR-8	HPA	1.548	0.113	0.073	0.12714	0.12679	0.350	-1.16	22.89	856	1.28
<i>Cape Searle</i>											
CS-7	HPA	0.484	0.506	1.044	0.13356	0.12844	5.03	1.06	20.18	831	1.47
dupl.	HPA	0.435	0.504	1.158	0.13442	0.12874	5.58	1.31	20.18	831	1.47
dupl.	CT	0.471	-	-	0.13369	-	-	-	20.18	831	1.47
<b>W.Greenland</b>											
<i>Anaanaa Member</i>											
400444	CT	1.907	0.259	0.136	0.12812	0.12746	0.655	0.23	20.81	769	1.53
400452	HPA	2.489	0.966	0.388	0.12922	0.12732	1.87	-0.72	21.55	913	1.49
400457	CT	3.879	0.359	0.093	0.12765	0.12720	0.446	0.02	22.65	848	1.40
400492	CT	2.533	1.140	0.450	0.13024	0.12804	2.17	0.70	20.05	801	1.57
408001.233	CT	1.503	0.243	0.162	0.12824	0.12746	0.779	0.22	17.99	751	1.45
<i>Naujanguit Member</i>											
113210	CT	3.119	0.206	0.066	0.12725	0.12693	0.318	-0.19	20.88	920	
264217	CT	2.786	0.472	0.169	0.12772	0.12689	0.816	-0.21	21.97	949	1.50
332771	CT	1.553	0.425	0.274	0.12837	0.12704	1.32	-0.10	20.09	824	1.57
362149	CT	2.813	0.291	0.103	0.12814	0.12759	0.550	0.33	23.45	1329	1.33
400485	HPA	4.024	0.316	0.079	0.12713	0.12674	0.378	-1.19	27.02	1184	1.17
<i>Ordlingassoq Member</i>											
113333	CT	2.256	0.063	0.028	0.12955	0.12942	0.134	1.77	20.53	935	
138228	CT	1.524	0.330	0.216	0.13321	0.13216	1.04	3.92	17.17	850	
332788	CT	2.034	0.180	0.089	0.13120	0.13094	0.427	2.97	25.62	1306	1.13
332828	CT	2.680	0.367	0.137	0.13060	0.12994	0.660	2.17	22.23	1098	1.35
332901	HPA	1.727	0.071	0.041	0.13123	0.13103	0.198	2.15	24.60	1098	1.22
354754	HPA	2.198	0.179	0.082	0.13254	0.13214	0.393	3.02	20.74	810	1.45
400230	HPA	2.768	0.335	0.121	0.13235	0.13175	0.584	2.72	21.77	935	1.43

Notes:

Reference materials analysed during the period of analysis (using HPA digestion) have been published previously in Dale et al. (2008) and Dale et al. (in review)

$^{187}\text{Os}/^{188}\text{Os}_i$  – Os isotope composition corrected for ingrowth of  $^{187}\text{Os}$  since the time of emplacement (61 Ma).

$\gamma\text{Os}$  – deviation of  $^{187}\text{Os}/^{188}\text{Os}_i$  from the chondrite evolution curve:  $((^{187}\text{Os}/^{188}\text{Os}_i / ^{187}\text{Os}/^{188}\text{Os}_{\text{chondrite}}) - 1) * 100$ .

Digestion method: HPA – high-pressure asher, CT – Carius tube, both digestions in inverse aqua regia.

Sample mass digested approx. 1g in all cases.

Figure 1

[Click here to download Figure: Fig 1 - MgO vs Os-Re.eps](#)

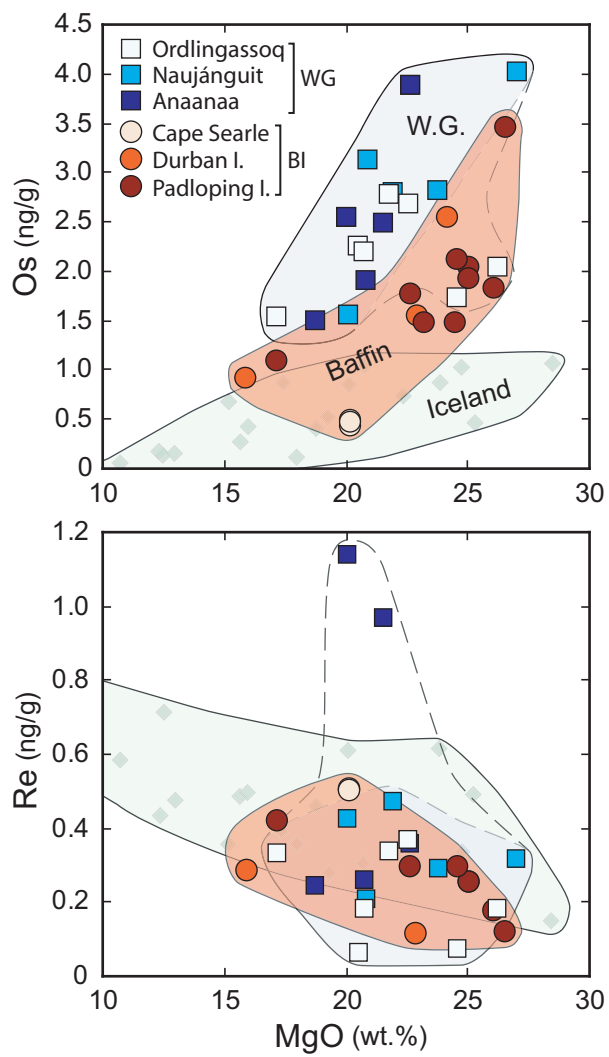
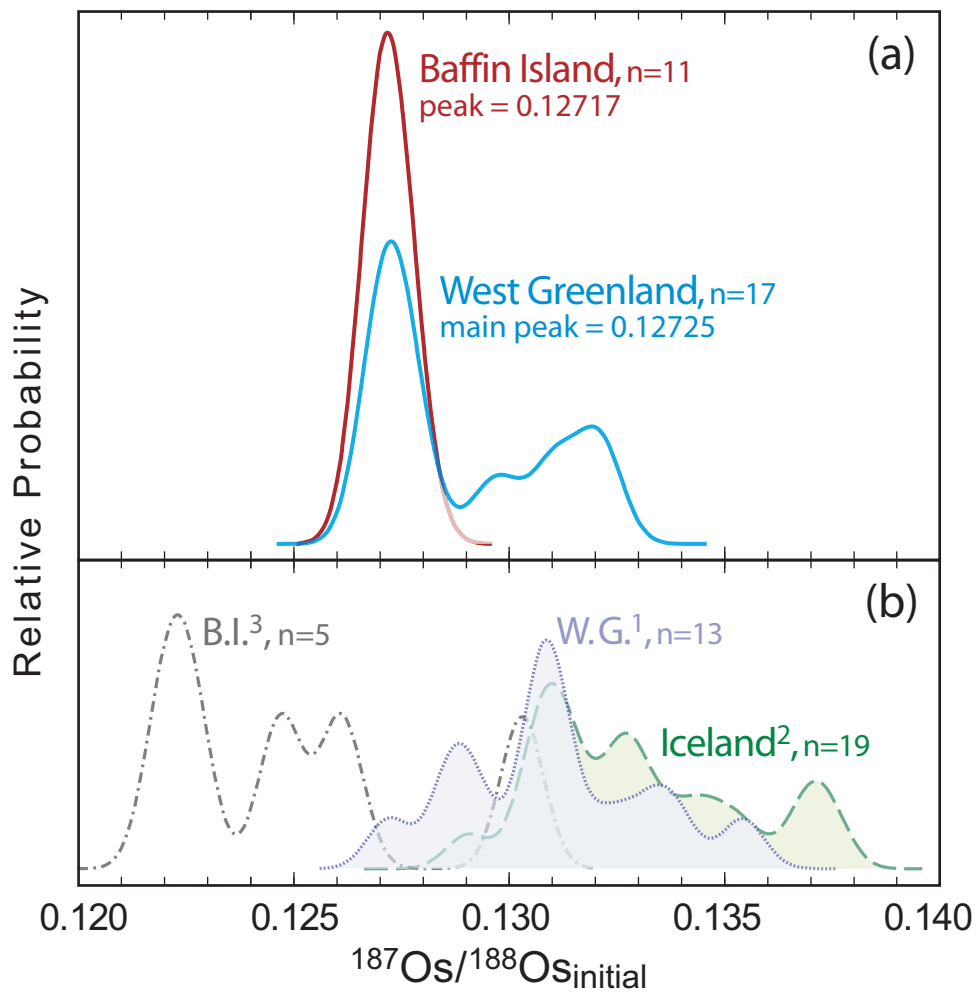


Figure 2

[Click here to download Figure: Fig 2 - New Os prob density new.eps](#)



**Figure 3**  
[Click here to download Figure: Fig 3 - Os v 187-188Os.eps](#)

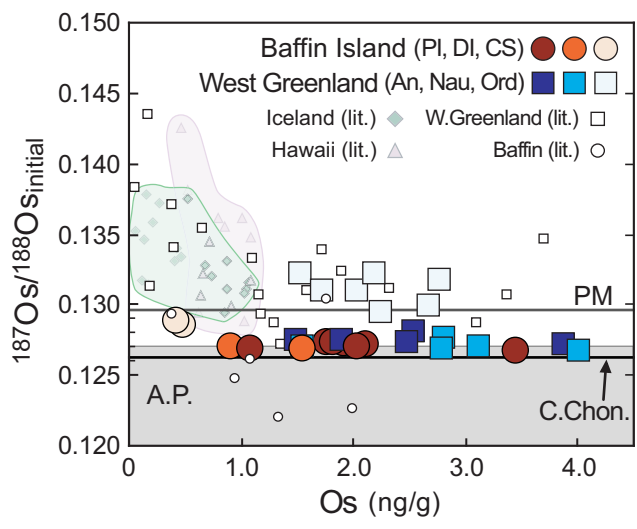


Figure 4

[Click here to download Figure: Fig 4 - 187-188Os v Nd.eps](#)

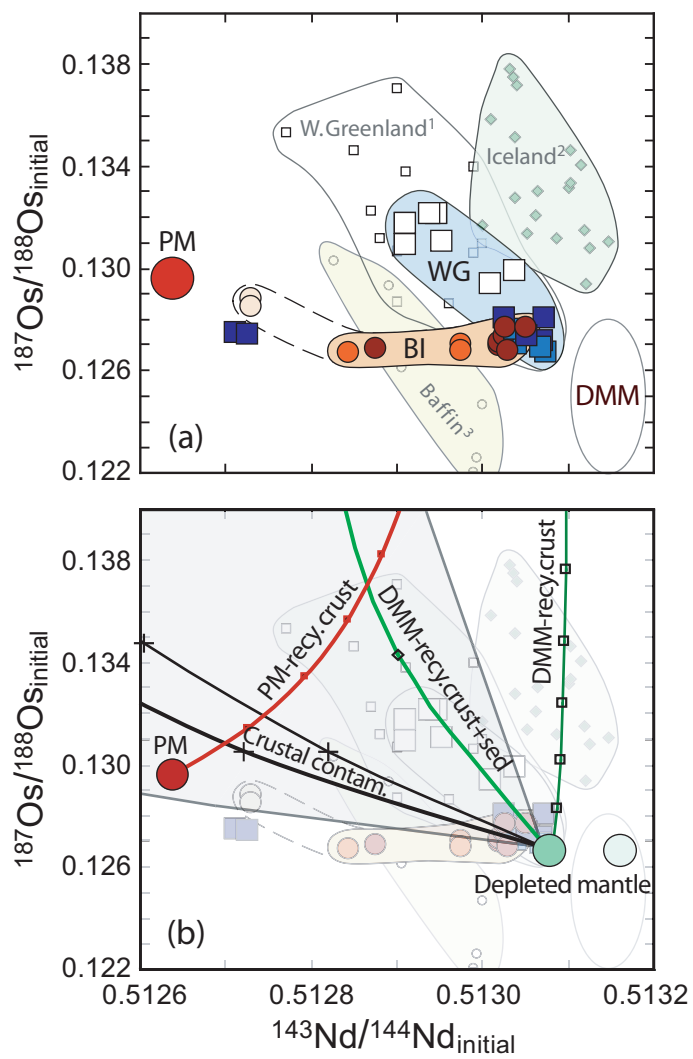


Figure 5

[Click here to download Figure: Fig 5 - New Os prob density new.eps](#)

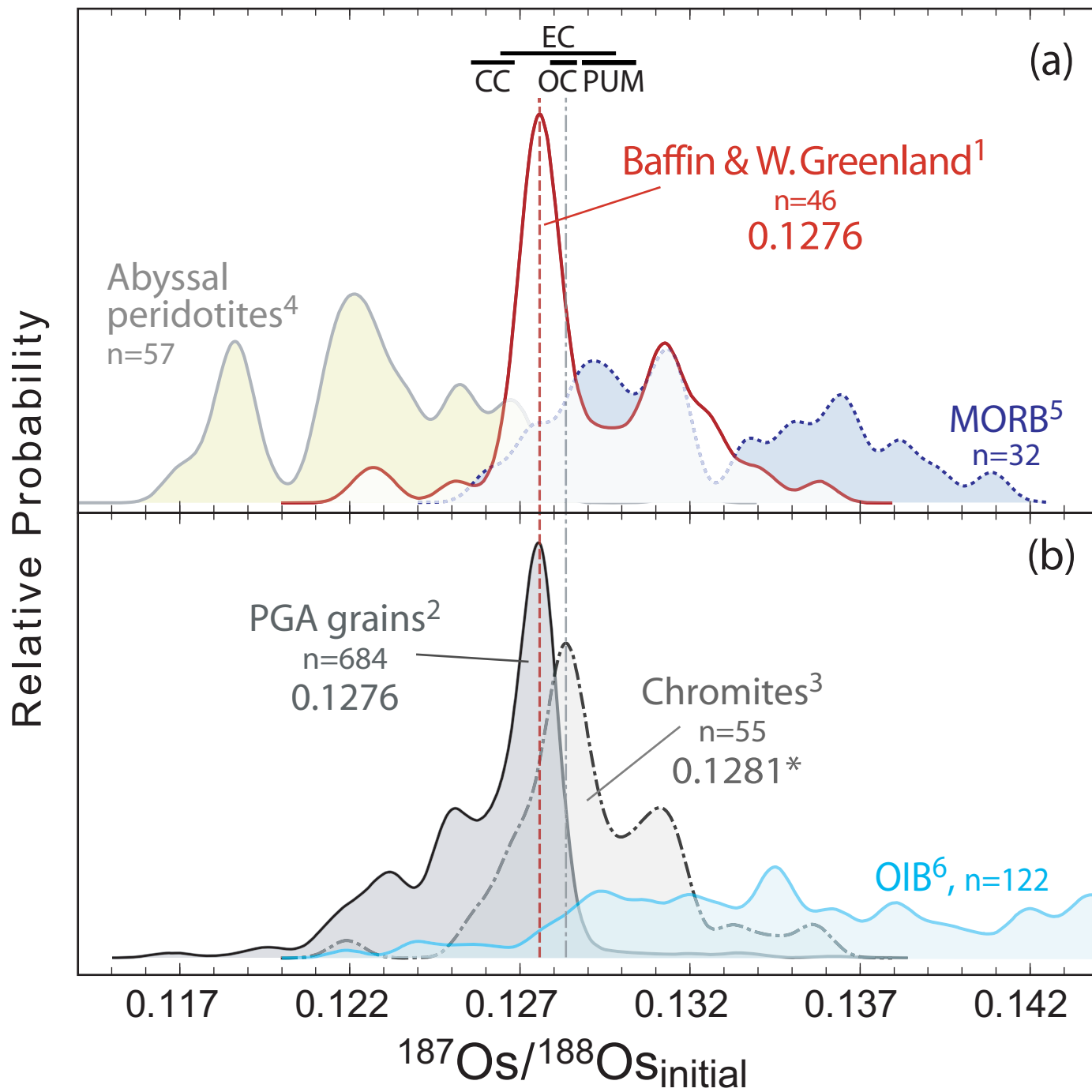


Figure 6

[Click here to download Figure: Fig 6 - 3-4He v 187-188Os & Os PDF.eps](#)

